Food and Chemical Toxicology 130 (2019) 122–129

Contents lists available at ScienceDirect

Food and Chemical Toxicology

journal homepage: www.elsevier.com/locate/foodchemtox

Transcriptional study after Beauvericin and Enniatin B combined exposure in Jurkat T cells

Laura Escrivá*[,1,2], Manuel Alonso-Garrido[1,2], Guillermina Font[2], Lara Manyes[2]

Laboratory of Food Chemistry and Toxicology, Faculty of Pharmacy, University of Valencia, Burjassot, Spain

ARTICLE INFO

Keywords:
In vitro
qPCR
Mitochondria
ToxPi
Beauvericin
Enniatin B

ABSTRACT

Simultaneous mycotoxins toxicity is complex and non-predictable based on their individual toxicities. Beauvericin and Enniatins are emerging mycotoxins highly co-occurrent in food and feed, and their cytotoxicity has been reported in several human cell lines. RNA-seq studies of individual exposure in Jurkat cells demonstrated human genome perturbation mainly affecting mitochondrial pathways, however, both mycotoxins showed differences between their toxic responses. This study investigates the transcriptional effects of combined exposure to Beauvericin and Enniatin B (1:1) (0.1, 0.5, 1.5 μM; 24 h) in Jurkat cells by qPCR on 30 selected target genes (10 mitochondrial, 20 nuclear). Gene expression after combined and individual exposures were compared and functional data analysis (ToxPi) on the most relevant biological processes (cycle and apoptosis regulation; cholesterol metabolism and transport; cellular signaling transduction; cellular stress responses; immune regulation; protein metabolism; retinoic acid metabolism; transcription regulation) was applied to RNA-seq data from individual exposure (1.5, 3, 5 μM; 24 h; Jurkat cells). Transcriptional changes, especially at mitochondrial level, were observed after Beauvericin-Enniatin B co-exposure including down-regulation of antioxidant activity related genes. Different expression patterns between combined and individual exposures were identified. ToxPi analysis confirmed different dose-dependent relationship profiles between these two mycotoxins after individual exposure.

1. Introduction

Mycotoxins worldwide occurrence in various food and feeds, as a consequence of the secondary metabolism of filamentous fungi, poses a major risk human and animal health (Smith et al., 2016). The simultaneous exposure to several mycotoxins is confirmed by both the co-occurrence of these toxins in food and feed stuff, and by co-exposure monitoring surveys being in practice the rule and not the exception (Stanciu et al., 2017). The toxicity of mycotoxins combinations is complex and it cannot always be predicted based upon their individual toxicities (Smith et al., 2016).

Beauvericin (BEA) and Enniatins (ENs) are cyclic hexadepsipeptides highly co-occurrent in food and feed since they are structurally related and produced by *Fusarium* species by the same metabolic pathway (EFSA, 2014). Grain-based food products are the most important contributors to the acute and chronic dietary exposure (Fraeyman et al., 2017). The cytotoxic effects of BEA and ENs has been demonstrated in several cell lines, including antibacterial, antifungal, insecticidal and phytotoxic activity, reactive oxygen species (ROS) production, lipid peroxidation (LPO), glutathione depletion and cell cycle alterations, which may result in apoptosis and/or necrosis (Mallebrera et al., 2016; Prosperini et al., 2017). However, the main mechanism of toxicity is considered to be related to their ionophoric properties which allow them to insert into the cell membrane, forming cation-selective pores and affecting cellular ionic homeostasis as well as uncoupling oxidative phosphorylation (Fraeyman et al., 2017).

Although the most commonly *in vitro* studied parameters in mycotoxin research are cell viability, apoptosis necrosis, DNA damage and oxidative stress (Smith et al., 2016), expression profiling of the entire transcriptome, which is highly dynamic and often responds sensitively to toxic exposure, may be considered as a sensitive early indicator of toxicity (Joseph, 2017). In this line, transcriptomic techniques allow the identification of genes whose expression levels are significantly affected after toxic exposure characterizing the responses to a toxic stimulus (Wilson et al., 2013).

The most common gene expression profiling techniques currently

* Corresponding author.
E-mail address: laura.escriva@uv.es (L. Escrivá).
[1] Both authors contributed equally to the manuscript.
[2] Postal address: Av. Vicent Andres Estelles s/n. 46100 Burjassot (Valencia) Spain.

https://doi.org/10.1016/j.fct.2019.05.018
Received 2 April 2019; Received in revised form 9 May 2019; Accepted 11 May 2019
Available online 14 May 2019

employed are quantitative real time PCR (qPCR), especially to determine the expression of limited number of transcripts, microarray analysis and next generation sequencing, the last two high throughput analysis techniques capable of determining expression levels of the entire transcriptome (Joseph, 2017).

In previous experiments, gene expression changes induced by BEA and EN B individual exposure (1.5, 3 and 5 μM; 24 h) in Jurkat cells were investigated through RNA-sequencing followed by differential gene expression analysis. BEA and EN B triggered perturbation up to 27% of human genome expression (5719 and 5750 genes), with 43 and 245 differentially expressed genes (DEGs) overlapped in all three studied concentrations for BEA and EN B, respectively. DEGs were mostly down-regulated belonging to biological processes and molecular functions related to mitochondrial respiration and metabolism. Pathway analysis revealed oxidative phosphorylation and electron transport chain as the most significantly altered pathways in all studied doses for both emerging mycotoxins (z-score > 1.96; adj p-value < 0.05), supporting scientific evidence that mitochondria is the main cell organelle responsible of BEA and EN B induced toxicity (Escrivá et al., 2018; Alonso-Garrido et al., 2018). However, these studies also revealed that the genome profile of BEA-exposed cells showed a concentration dependent alteration leading to mitochondrial affection and apoptosis through the caspase cascade activation, while EN B exposure also led to significant differences in DEGs number between the two highest concentrations compared to the lowest one, discarding the linear dose dependence, and only mitochondrial alteration was detected but no apoptosis tendency.

Differences in toxic responses observed after BEA and EN B exposure in Jurkat T-cells were also reported in cytotoxicity studies based on common endpoints, where BEA mediated cytotoxicity through mitochondrial alterations highly affecting cell cycle and reaching a point of no-recovery with apoptotic and apoptotic/necrotic cells increase, while EN B effects were only observed at high concentrations and times assayed being not such evident than for BEA exposure. Although both mycotoxins enhanced the number of caspase activated cells, DNA damage revealed that only BEA at high concentrations (3 and 5 μM) was involved in genotoxic effects (Manyes et al., 2018).

To gain more information about the effects at transcriptomic level after the combined exposure to BEA and EN B in Jurkat T-cells, a transcriptional study based on qPCR focused on selected target genes was designed.

2. Material and methods

2.1. Reagents

The reagent grade chemicals and cell culture components used: RPMI-glutamax medium, penicillin/streptomycin, Fetal Bovine Serum (FBS), phosphate buffer saline (PBS), BEA (783.95 g/mol, 97% purity) and EN B (783.95 g/mol, 97% purity) were purchased by Sigma chemical Co. (St. Louis, MO, USA).

Dimethyl sulfoxide (DMSO) and methanol were obtained from Fisher Scientific (Madrid, Spain). Deionized water (resistivity < 18 MV cm) was obtained using a Milli-Q water purification system (Millipore, Bedford, MA, USA). Stock solutions of BEA and EN B (1 mg/ml) were prepared in methanol and maintained at −20 °C. Final concentrations of mycotoxins in the assay were achieved by their dilution in the culture medium. The final DMSO concentration in the medium was 0.5% (v/v).

2.2. Cell culture and mycotoxins exposure

Jurkat T-cells derived from human T lymphocyte peripheral blood were maintained in RPMI-glutamax medium supplemented with 100 U/mL penicillin, 100 mg/mL streptomycin and 10% (v/v) FBS inactivated. Incubation conditions were pH 7.4, 37 °C under 5% CO2 and 95% air atmosphere at constant humidity. Culture medium was changed every two days. Absence of mycoplasma was checked routinely using the Mycoplasma Stain Kit (Sigma Aldrich, St Louis Mo. USA). Before contamination, cells were plated in 12-well tissue culture plates at a density of 5×10^5 cells/well. Jurkat T-cells were then co-exposed for 24 h to BEA-EN B (0.1 μM, 0.5 μM, and 1.5 μM) in 0.5% DMSO and the solvent concentration as control (each condition n = 3) in maintenance medium and standard conditions. Mycotoxin concentrations were chosen to simulate a realistic scenario (Table 1).

Table 1
Relation between food contamination levels and plasma concentration (Devreese et al., 2013; Korkalainen et al., 2017).

Plasma concentration (μM)	Food contamination (μg/kg)	
	BEA	EN B
0.1	78	64
0.5	390	320
1.5	1170	960
3	2340	1920
5	3900	3200

2.3. RNA extraction and quantification

Total RNA of the control and exposed Jurkat T-cells was isolated using ReliaPrep™ RNA Cell Miniprep System kit and treated with RNase free DNase (Promega) to remove genomic DNA contamination. The extracted RNA of each sample was firstly checked for quantity and quality using Nanodrop2000 (Thermo Scientific), showing concentrations between 140 and 152 ng/μl and appropriate 260/280 and 260/230 ratios both around 2. RNA samples were stored at −20 °C until their dilution to 100 ng/μl with pure Milli-Q H20 until their reverse transcription to cDNA.

2.4. Genes selection and primers design

Potential candidate genes for the study were selected based on previous results of RNA-sequencing data after individually exposure of Jurkat T-cells to BEA and EN B. The selected candidate genes included 10 mitochondrial genes since they were the 9 most strongly down-regulated genes plus the most strongly up-regulated one (Escrivá et al., 2018; Alonso-Garrido et al., 2018). The mitochondrial genes included MT-ND2, MT-ND3, MT-ND4, MT-ND4L, MT-ND5, MT-CO1, MT-CO3, MT-ATP6, MT-ATP8, MT-RNR2 and MRPL12.

To cover wider genome alterations along with those related to mitochondrial genes, 20 nuclear genes were selected belonging to different functional categories such as uncoupling proteins (UCP2 and UCP3), cell metabolism (ABCA1, ABCG1, AK4), cell cycle (CCNG2), cell signaling (CEBPB, GPR18), cell transport (HSPA5, SLC7A11, SRXN1), cell differentiation (ID2, VPREB1), enzyme activity (CRIM1), biosynthesis (HMGCS1), immune system (IL-32), oxidoreductase activity and oxidative stress (NQO1, OSGIN1), and redox signaling (TXNIP). 18S rRNA, already validated as an appropriate reference gene, was used for normalization (Banda et al., 2008).

Primer pairs for each gene were designed based on the entire coding region of the candidate genes using Primer-BLAST (Ye et al., 2013) according to the following parameters: primer length of about 20 bases, GC content of 45–60%, melting temperature (Tm value) between 58 and 59 °C, and amplicon product size ranging from 50 to 150 base pair.

2.5. Reverse transcription, qPCR reactions and relative quantification

First, cDNA was synthesized using 5 μL of total RNA (500 ng) according to the instructions of TaqMan™ MicroRNA Reverse Transcription Kit protocol (Thermo Fisher Scientific, Spain). cDNA was

Table 2
Gene symbol, gene name, optimum qPCR temperatures, forward and reverse primers, product length, efficiency and linearity of the selected genes plus the reference gene.

Gene Symbol	Gene Name	Optimum Temp. (C°)	Forward Primer/Reverse Primer	Efficiency (%)	Linearity (R^2)
ABCA1	ATP binding cassette subfamily A member 1	58.5	GGAGAGCACAGGCTTTGACC/GCTCGCAATTACGGGGTTTTT	123.4	0.988
ABCG1	ATP binding cassette subfamily G member 1	58.5	GTCAAGGACAATGTGTGTAC/GTCTCTCTTGTGGTCTGAGT	117.0	0.980
AK4	adenylate kinase 4	58.5	CTTTGAGTCACCCCCGCTT/TCCTTAACTCCAGCTCGCTC	143.4	0.988
CCNG2	cyclin G2	59	AGGTGAGGCTACAGTGATTCC/AGGCACAGATGCCAAACCTA	95.4	0.991
CEBPB	CCAAT/enhancer binding protein beta	58.5	GGCCGGTTTCGAAGTTGATG/CAGTTACACGTGGGTTGCG	128.7	0.991
CRIM1	cysteine rich transmembrane BMP regulator 1	59	GGTTCCTGTTGTGCTCTTGTAA/TGCCAAGAATCAAGTTGCAGAT	132.8	0.981
GPR18	G protein-coupled receptor 18	58.5	GGCCATTTGGAGAGTACTTC/GGGAGTGGAGTCTTTATCTG	151.1	0.979
HMGCS1	3-hydroxy-3-methylglutaryl-CoA synthase 1	58.5	TCTCCATACAGTGCTACCTC/GCCTTCTCCACATCTCTATC	144.2	0.984
HSPA5	heat shock protein family A (Hsp70) member 5	58.5	TTTCTGAGACCCTGACTCGG/AGACCGGAACAGATCCATGT	113.5	0.99
ID2	inhibitor of DNA binding 2	59	GACCACCCTCAACACGGATA/ATGAACACCGCTTATTCAGCC	129.2	0.996
IL32	Interleukin 32	59	CCTCAGACCCCTTGTGAAGC/GCCCTTGAATCTTCTACGAACC	110.1	0.989
MRPL12	mitochondrial ribosomal protein L12	58	GATGGGTGGTGTGATGTCTG/TGTCCGTTCTTTCGCTATGG	123.8	0.992
MT-ATP6	mitochondrially encoded ATP synthase membrane subunit 6	58	TTCGCTTCATTCATTGCCCC/TGGGTGGTGATTAGTCGGTT	76.4	0.985
MT-ATP8	mitochondrially encoded ATP synthase membrane subunit 8	58.5	CCCTGAGAACCAAAATGAACGA/GATTGTGGGGGCAATGAATGA	112.9	0.996
MT-CO1	mitochondrially encoded cytochrome *c* oxidase I	58	TCATAATCGGAGGCTTTGGC/GTTGTTTATGCGGGGAAACG	121.1	0.992
MT-CO3	mitochondrially encoded cytochrome *c* oxidase III	58	CTTCCACTCCATAACGCTCC/GTTACATCGCGCCATCATTG	129.6	0.991
MT-ND2	mitochondrially encoded NADH: ubiquinone oxidoreductase core subunits 2	58	CGTAAGCCTTCTCCTCACTC/CAACTGCCTGCTATGATGGA	141.3	0.997
MT-ND3	mitochondrially encoded NADH: ubiquinone oxidoreductase core subunits 3	58	GACTACCACAACTCAACGGC/GGGCTCATGGTAGGGGTAAA	82.0	0.996
MT-ND4	mitochondrially encoded NADH: ubiquinone oxidoreductase core subunits 4	58	CACACGAGAAAACACCCTCA/AAACCCGGTAATGATGTCGG	151.9	0.992
MT-ND4L	mitochondrially encoded NADH: ubiquinone oxidoreductase core subunits 4L	58.5	CCCACTCCCTCTTAGCCAAT/GGCGGCAAAGACTAGTATGG	121.0	0.993
MT-ND5	mitochondrially encoded NADH: ubiquinone oxidoreductase core subunits 5	58	CATCCCCCTTCCAAACAACA/GTCCTAGGAAAGTGACAGCG	125.2	0.991
MT-RNR2	mitochondrially encoded 16S RNA	58	GGTGCAGCCGCTATTAAAGG/ATCATTTACGGGGGAAGGCG	85.5	0.991
NQO1	NAD(P)H quinone dehydrogenase 1	58.5	GTTTGGAGTCCCTGCCATTC/CCTTCTTACTCCGGAAGGGT	113.8	0.99
OSGIN1	oxidative stress induced growth inhibitor 1	58	TCTTTGATGCCCTTCTACGC/CGACTTCATGTTTCCCCCAA	142.9	0.98
SLC7A11	solute carrier family 7 member 11	58	ATGCAGTGGCAGTGACCTTT/CATGGAGCCAAAGCAGGAGA	128.1	0.958
SRXN1	sulfiredoxin 1	58	GGTCTAGGGGAAGAGGTGTT/CTTGGTTTTCAGAAGCCCCT	137.5	0.992
TXNIP	thioredoxin interacting protein	58	GTGAAGGTGATGAGATTTCC/CTCTGACTGATGACAACTTC	125	0.985
UCP2	uncoupling protein 2	58	AAAGGTCCGATTCCAAGCTC/TTTGGTATCTCCGACCACCT	122.5	0.989
UPC3	uncoupling protein 3	58.5	GGAACGTGGTGATGTTCGTA/AAACGGTGATTCCCGTAACA	127.3	0.982
VPREB1	V-set pre-B cell surrogate light chain 1	58.5	GTCTACTGCACAGGTTGTGG/CGATGTCATGGTCGTTCCTC	144.4	0.991
18S rRNA	18S ribosomal RNA	58	CGGCTACCACATCCAAGGAA/GCTGGAATTACCGCGGCT	105.0	0.994

subsequently stored at −20 °C until use for qPCR reactions. qPCR was performed for all primer pairs and a single amplification product was obtained for each gene by the melting curve assay. Primer amplification efficiency was determined from standard curve generated by cDNA serial dilution (2 fold each) for each gene in triplicate. Correlation coefficients (R^2) and amplification efficiencies (E) for each primer pairs were calculated from slope of regression line by plotting mean Cq values against the log cDNA dilution factor in StepOne software (Table 2). Real-time amplification reactions were performed in 96 well plates using SYBR Green detection reactive and run in triplicate on 96-wells plates with the StepOne Plus Real-time PCR instrument (Applied Biosystems). Reactions were prepared in a total volume of 10 μl containing: 3 μl of 1:2 diluted template, 2 μl of amplification primer mix (forward/reverse of each gene) (2.5 μM) and 5 μl of 2 × Fast SYBR Green (Applied Biosystems). Non-template controls (NTC) were also included for each primer pair, replacing the template by DNAse and RNAse free water from the RNA extraction kit.

The cycling conditions were set as default: initial denaturation step of 95 °C for 5 min to activate the Taq DNA polymerase, followed by 40 cycles of denaturation at 95 °C for 15 s, annealing temperatures ranging from 58 to 59 °C (depending on the primers) for 15s and elongation at 72 °C for 45s. The melting curve was generated by heating the amplicon from 60 to 90 °C. Baseline, threshold cycles (Ct) and primer parameters analysis were automatically determined using the StepOne Plus Software version 2.3 (Applied Biosystems). All the experiments were done according to MIQE (Minimum Information for Publication of Quantitative Real-Time PCR Experiments) guidelines[32].

2.6. Statistical analysis

In order to assess the statistical analysis, normalized Cp calculated as ΔCp (experimental Cp -housekeeping Cp mean) obtained by qPCR was used. Student test was applied to evaluate differences between groups. Statistical analysis was performed with SPSS 24.0 (IBM Corp., Armonk, NY, USA). $p < 0.05$ was considered to indicate a statistically significant difference.

2.7. Bioinformatics

ToxPi interactive software tool was used to compare the modes of action of the compounds[33]. Gene selection was based on previous findings in immunotoxic gene signature[12]. ToxPi score (0–1) was calculated for each individual mycotoxin exposure on each different functional GO by dividing the results obtained on the genes involved in the GOs after each exposure condition (BEA 1.5 μM; BEA 3 μM; BEA 5 μM; EN B 1.5 μM; EN B 3 μM; EN B 5 μM) by the maximum results on the same genes from all the exposure conditions. Hierarchical clustering was completed with the programs Cluster (uncentered correlation; average linkage clustering) and Treeview[34]. Red and green indicate up- and down-regulation vs. average expression of control samples.

3. Results

3.1. Gene expression analysis

The expression of the 30 genes studied after BEA and EN B co-exposure in Jurkat cells was determined by qPCR. Cp values and significant differences compared with vehicle control are summarized in Table 3.

As it can be observed, MT-CO1 and CO3 were up-regulated while the other mitochondrial genes checked did not show a clear pattern. Except these two genes, all of them were slightly altered, up- or down-regulated depending on the concentration, less than 1-fold change compared to control. On the contrary, nuclear gene expression was less altered than mitochondrial but it showed three different shapes. CEBPB, UCP2, UCP3, ABCG1, MRPL12, OSGIN1, CCNG2, CRIM1 and IL-32 were down-regulated in a concentration-dependent manner; SLC7A11, NQO1, HMGCS1, VPREB1, ABCA1, AK4 and ID2 were slightly down-regulated at the three studied concentrations but their expression was not correlated with dose; GPR18, SRXN1 and HSPA5 were to some extent down- or up-regulated. Finally, TXNIP showed a little up-regulation in a concentration-dependent manner. Although not all the results were statistically significant (Table 3), altered expression was constant among biological replicates.

3.2. Mixture vs. individual mycotoxin exposure

A comparison between mixture exposure results by qPCR and those obtained from individual Jurkat cells exposure to BEA or EN B by RNA sequencing is shown in Fig. 1. In first place, it can be perceived that mixture exposure at low concentrations triggered smaller expression changes in the selected genes than the studied individual exposure concentrations, which is in accordance with the previous tendency observed in the individual mycotoxin contamination results, especially when using BEA (Manyes et al., 2018; Escrivá et al., 2018).

Mitochondrial gene expression in mixture exposed cells does not follow a clear profile while it does in individual exposed ones; nevertheless, slender up-regulation predominates for all genes but MT-ND4L and MT-RNR2. MT-CO1 and 3 gene expressions are the most unlike comparing individual and combined exposures, where they appear down- and up-regulated, respectively. On the lower part of Fig. 1, MT-RNR2 shows a tendency to be up-regulated at all treatments excluding the lowest mixture concentrations used, where a slight down-regulation appears.

Regarding nuclear genes, the opposite expression trend continued between mixture and individual exposed cells. Whereas gene transcription down-regulation prevailed after mixtures exposure at low levels, apart from TXNIP (Table 3), individual exposure was followed by up-regulation (Fig. 1).

3.3. ToxPi results

Functional data analysis performed by ToxPi software/US EPA was focused on specific biological processes and molecular functions based on the most relevant Gene Ontology (GO) annotations in which the studied genes were involved (Fig. 2). The selected relevant GOs were in agreement with previous immunotoxicological transcriptomic studies (Shao et al., 2014). GOs are listed as follows: regulation of cell cycle and apoptosis; metabolism and transport of cholesterol; cellular signaling transduction; cellular stress responses; immune regulation; protein metabolism; retinoic acid metabolism; and regulation of transcription.

The expression level of the 30 studied genes after BEA and EN B individual exposure to human Jurkat T cells was obtained from previous NGS transcriptomic experiments recently carried-out by the research group (Escrivá et al., 2018; Alonso-Garrido et al., 2018). BEA:EN B mixture exposure results were not included because of the small fold changes obtained.

As it is shown in Fig. 2, the pattern observed after the exposure to the highest EN B concentrations (3 and 5 μM) were considerably similar between them but quite far from the lowest concentration (EN B 1.5 μM). Indeed, the highest EN B doses reached the maximum ToxPi score (1) in 7 out of the 8 studied GOs: regulation of cell cycle and apoptosis, metabolism and transport of cholesterol, cellular stress responses, regulation of transcription (5 μM); cellular signaling transduction, immune regulation, and retinoic acid metabolism (3 μM). However, ToxPi scores at the lowest EN B concentration were below 0.45 for all the studied GO annotations.

With regard to BEA exposure, relevant ToxPi scores were observed at the highest concentration (5 μM) for protein metabolism (1), cellular signaling transduction (0.96), regulation of cell cycle and apoptosis (0.86), and cellular stress responses (0.84); while values were lower than 0.76 after BEA 3 μM and no score at all at the lowest concentration

Table 3
qPCR results triggered by BEA:EN B exposure during 24 h in Jurkat cells. Average expression of genes normalized Cp ± standard deviation and log2RQ. *p < 0.05, **p < 0.01 and ***p < 0.001 compared with the control. RQ, relative quantity. log2RQ C control = 0. Cp norm = normalized Cp using reference gene results.

Gene	Control	0.1 μM		0.5 μM		1.5 μM	
	Cq norm	Cq norm	log2RQ	Cq norm	log2RQ	Cq norm	log2RQ
ABCA1	21.72 ± 0.01	20.56 ± 0.36	−0.08	21.53 ± 0.02	−0.01	**17.86 ± 0.30***	−0.28
ABCG1	15.85 ± 0.23	15.34 ± 0.50	−0.05	14.15 ± 0.13	−0.16	**13.99 ± 0.19***	−0.18
AK4	16.84 ± 0.24	**15.20 ± 0.35***	−0.15	**13.68 ± 0.11***	−0.30	16.05 ± 0.12	−0.07
CCNG2	19.10 ± 0.19	**18.60 ± 0.11****	−0.04	**18.07 ± 0.13***	−0.08	16.67 ± 0.11	−0.20
CEBPB	12.60 ± 0.35	12.18 ± 0.31	−0.05	**10.75 ± 0.19****	−0.23	**9.99 ± 0.06****	−0.34
CRIM1	18.04 ± 0.03	17.62 ± 0.21	−0.03	17.20 ± 0.35	−0.07	**16.08 ± 0.12***	−0.17
GPR18	14.00 ± 0.02	14.24 ± 0.26	0.03	12.96 ± 0.20	−0.11	**11.87 ± 0.03***	−0.24
HMGCS1	13.23 ± 0.06	**11.32 ± 0.20***	−0.22	**11.40 ± 0.00***	−0.22	**10.60 ± 0.07***	−0.32
HSPA5	8.56 ± 0.46	9.45 ± 0.63	0.14	6.26 ± 0.11	−0.45	**6.72 ± 0.06****	−0.35
ID2	12.95 ± 0.06	12.30 ± 0.08	−0.07	12.03 ± 0.14	−0.11	12.19 ± 0.06	−0.09
IL-32	13.47 ± 0.02	13.26 ± 0.17	−0.02	**12.50 ± 0.07****	−0.11	12.34 ± 0.22	−0.13
MRPL12	9.83 ± 0.21	9.30 ± 0.29	−0.08	8.99 ± 0.09	−0.13	**8.70 ± 0.20****	−0.18
MT-ATP6	2.20 ± 0.09	3.92 ± 0.56	0.14	1.81 ± 0.16	−0.65	**3.62 ± 0.03***	0.56
MT-ATP8	2.26 ± 0.05	2.48 ± 0.03	0.83	**1.43 ± 0.05***	−0.28	**3.33 ± 0.10***	0.72
MT-CO1	1.27 ± 0.12	**1.89 ± 0.15***	0.57	**4.96 ± 0.01***	1.96	**4.72 ± 0.12***	1.89
MT-CO3	1.18 ± 0.20	2.24 ± 0.45	0.92	2.27 ± 0.12	0.94	1.96 ± 0.02	0.73
MT-ND2	4.23 ± 0.07	4.31 ± 0.03	0.02	**2.94 ± 0.08****	−0.53	4.71 ± 0.44	0.15
MT-ND3	2.46 ± 0.07	2.97 ± 0.09	0.27	2.14 ± 0.13	−0.20	**4.40 ± 0.03***	0.84
MT-ND4	2.26 ± 0.18	1.93 ± 0.44	−0.23	2.74 ± 0.12	0.27	**4.23 ± 0.08***	0.90
MT-ND4L	4.92 ± 0.45	5.22 ± 0.57	0.09	3.34 ± 0.08	−0.56	2.73 ± 0.12	−0.85
MT-ND5	6.12 ± 0.16	6.81 ± 0.18	0.15	**4.60 ± 0.13****	−0.41	6.63 ± 0.11	0.11
MT-RNR2	2.42 ± 0.05	**1.80 ± 0.00***	−0.43	**1.76 ± 0.02***	−0.46	**3.36 ± 0.12***	0.47
NQO1	9.95 ± 0.04	**8.77 ± 0.12***	−0.18	8.93 ± 0.40	−0.16	**8.37 ± 0.03*****	−0.25
OSGIN1	15.24 ± 0.14	14.87 ± 0.02	−0.04	**14.19 ± 0.14****	−0.10	**13.33 ± 0.05***	−0.19
SLC7A11	17.27 ± 0.22	15.89 ± 0.01	−0.12	15.68 ± 0.31	−0.14	15.66 ± 0.03	−0.14
SRXN1	11.88 ± 0.03	12.10 ± 0.21	0.03	**10.86 ± 0.08***	−0.13	**10.94 ± 0.28***	−0.12
TXNIP	8.60 ± 0.35	8.58 ± 0.03	0.00	8.94 ± 0.24	0.06	10.10 ± 0.03	0.23
UCP2	9.10 ± 0.13	8.76 ± 0.06	−0.05	7.58 ± 0.16	−0.26	**7.38 ± 0.03***	−0.30
UCP3	20.79 ± 0.42	**19.61 ± 0.38***	−0.08	**18.29 ± 0.34***	−0.19	17.80 ± 0.11	−0.22
VPREB1	22.30 ± 0.62	20.74 ± 0.33	−0.10	18.01 ± 0.01	−0.31	20.44 ± 0.24	−0.13

(1.5 μM).

4. Discussion

The qPCR study carried out shows how *Fusarium* mycotoxins BEA and EN B induce transcriptional alterations in Jurkat cells at low concentrations which represent realistic scenarios (Table 1). It is important to highlight that the European Food Safety Authority highest mean acute exposure estimate in Europe is 0.05 μg BEA/kg body weight (bw) per day and 4.67 μg EN/kg bw/day for toddlers. Toddlers have been described as the age cluster with the highest dietary chronic and acute exposure to both BEA and the sum of ENs (EFSA 2014). A toddler of 10 kg in Europe may have an intake of 46.7 μg EN and 0.5 μg BEA per day.

Regarding the genes whose proteins form the electron transport chain (Table 3), higher expression alteration was observed than in nuclear genes but no pattern can be suggested except for MT-CO1 and 3 that were slightly up-regulated. MT-CO1, the most up-regulated of these two genes, has been related to enhanced mitochondrial oxidative phosphorylation, allowing cells to produce high amounts of ATP (Whitaker-Menezes et al., 2011). The immune synapse is where cell signaling occurs between T cell and an antigen-presenting cell. Mitochondria are carried to the synapse following their interaction with matching antigen-presenting cells and are intentionally localized there because polarization of different structures and transport of ions across membranes necessitate energy delivered as ATP (Quintana et al., 2012).

On the contrary, the expression of eight nuclear genes (ABCG1, IL-32, CEBPB, MRPL12, OSGIN1, UCP2, UCP3, CCNG2, and CRIM1) associated with oxidative stress processes was slender down-regulated in a concentration-dependent manner and TXNIP, up-regulated (Table 3). Interestingly, it has been seen that ABCG1 regulates T cell differentiation into Tregs, highlighting a pathway by which cholesterol accumulation can influence T cell homeostasis in atherosclerosis (Cheng et al., 2016). Moreover, it has been reported a role for IL-32 in cholesterol transporters regulation and a direct influence in ABCA1 and ABCG1 mRNA levels, in agreement with results shown in Table 3 (Damen et al., 2018). About the other mentioned genes, CEBPB down-regulation can affect the differentiation of T-cells and the activation of the immune and inflammatory responses (Pan et al., 2014). CCNG2 blocks cell cycle entry thought activation of PI3K (Martínez-Gac et al., 2004). Recently, it has been confirmed that reduction of membrane protein CRIM1 decreases e-cadherin and increases claudin-1 and MMPs, enhancing the migration and invasion of renal carcinoma cells (Ogasawara et al., 2018). MRPL12 belongs to a set of ribosomes needed to translate the 13 mtDNA-encoded mRNAs involved in oxidative phosphorylation (Nouws et al., 2016). OSGIN1 together with p53 is involved in regulating mitochondrial structure and function (Hu et al., 2012). UCP2 has highly important roles in mediating ROS production and regulating apoptosis and autophagy, as well as maintaining gap junction integrity and progesterone in cumulus cells synthesis (Ge et al., 2017). UCP3 is located with UCP2 in the mitochondrial membrane and its expression is associated with body mass index, percentage of lean body mass, and percentage of mass in the postoperative period (Oliveira et al., 2017).

Cells individually exposed to both BEA and EN B at high concentrations showed a clear down-regulation of the mitochondrial genes highlighting a great relevance to mitochondria as a target site (Alonso-Garrido et al., 2018; Escrivá et al., 2018). Analyzing these results, it can be suggested that BEA:EN B mixture at low levels in Jurkat cells provokes a more dangerous transcriptomic profile than the individual exposure of these mycotoxins because it upregulates CO1 and 3 which will provoke more ROS generation than normal conditions. In addition, it down-regulates the expression of antioxidant-activity related genes (ABCG1, IL-32, CEBPB, MRPL12, OSGIN1, UCP2, UCP3, CCNG2, and CRIM1) among other important cell functions. This could lead to an impaired immune function because ROS balance in T cells must be strongly regulated during antigen activation (Zhang et al., 2016).

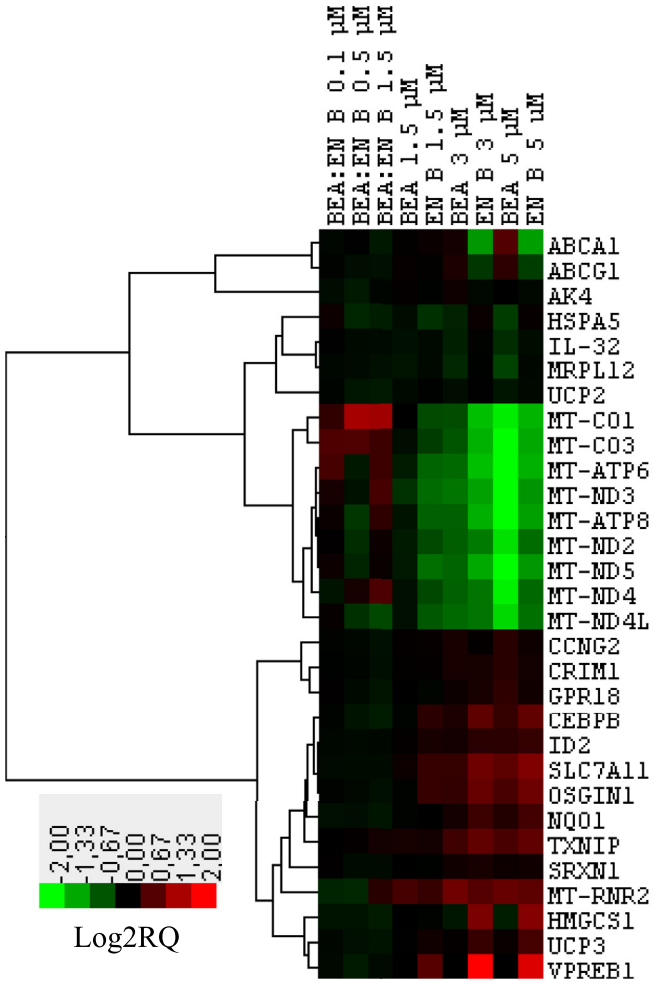

Fig. 1. Hierarchical clustering of the mRNA expression levels of 30 genes tested in human Jurkat T cells exposed to BEA and EN B (0.1, 0.5 and 1.5 µM; 24 h). Values represent the average ± SD of technical triplicates. Each compound was tested in three independent biological replicates. Color scale represents log2 ratios vs. vehicle control. Red indicates gene up-regulation, while green indicates down-regulation. RQ, relative quantification. (For interpretation of the references to color in this figure legend, the reader is referred to the Web version of this article.)

The available information on the human genome alteration induced by BEA and EN B is limited, and there are no previous studies evaluating the effects of BEA:EN B co-exposure at transcriptional level. However, some individual exposure transcriptome studies by microarrays and qPCR have been performed in different cell lines. Expression of genes related to ABC transporter activity (ABCB1, ABCG2), mitochondrial function (MT-CO1) and apoptosis (BAX, BCL2, CASP3) was evaluated by qPCR in cumulus cells and oocytes after BEA exposure (10 µM; 22–44 h). Increased expression of ABCB1, ABCG2 and BCL2 in cumulus cells, and increased MT-CO1 expression in oocytes was discovered. Authors concluded that mitochondrial function was altered by BEA exposure in oocytes without signs of apoptosis pathways activation (Schoevers et al., 2016).

The mechanism of toxicity of EN B (1–20 µM; 4 h) was assessed by microarrays in rat primary hepatocytes revealing 37 down-regulated genes involved mitochondrial organization, highlighting genes associated with apoptosis and cell signal transduction. Genome profiling revealed altered mitochondrial organization and dysfunction of the mitochondrial electron transport chain due to effects on function and assembly of complex I, with alteration of the energy metabolism. Authors suggested EN B as acting through energy deprivation due to mitochondrial alteration in HepG2 and Balb 3T3 cells, and by necrotic cell death in primary cells (Jonsson et al., 2016).

Proinflammatory interactions between the multiple microbial agents were studied in macrophages derived from human THP-1 monocytic cells after EN B (5 µM; 24 h) exposure. Expression of proinflammatory cytokines (TNFa and IL-1b) was slightly altered inducing mitochondrial damage and autophagocytosis with β-glucan and lipopolysaccharides co-exposure. Both co-exposures synergistically increased the expression levels of several inflammation-related genes, as well as induced inhibitory effects in some of the responses indicating that effects on immune system largely depend on substances combinations and their concentrations, which hinder the prediction of total exposure consequences (Korkalainen et al., 2017).

Recently, transcription levels were evaluated by qPCR in mice blastocysts after parents EN B1 intravenously administration (1, 3, and 5 mg/kg/d) prior matting, showing down-regulation of genes related to innate immunity (IL-8, IL-1β and CXCL1), and suggesting the potential of EN B1 to exert cytotoxic effects on embryos as well as, oxidative stress and immunotoxicity during mouse embryo development (Huang et al., 2018).

In previous studies for the identification and validation of genomic human immunotoxicity biomarkers, some mycotoxins were tested at sub-cytotoxic doses in Jurkat T cells and gene expression levels of 25 genes -including 15 common genes in the present study-were assessed by qPCR. Although the emerging mycotoxins were not included, the *Fusarium* mycotoxin Zearalenone revealed cellular stress response, immune regulation, regulation of cell cycle and apoptosis, and regulation of transcription as the main representative GOs based on the ToxPi scores (Schmeits et al., 2017), while the most relevant GO annotations for Ochratoxin A included cellular signal transduction, regulation of transcription, and retinoic acid metabolism (Shao et al., 2014). When comparing both mycotoxins in ToxPi (Fig. 2), higher intensities for the studied GOs were observed for EN B, however common representative biological processes were identified for both mycotoxins at the highest concentrations (5 µM): regulation of cell cycle and apoptosis, and cellular stress responses as Zearalenone, and cellular signaling transduction as Ochratoxin A. These relevant processes are in agreement with recent investigations in Jurkat cells which showed cell cycle arrest in S phase and a decrease in the cells percentage in G2/M stage for both mycotoxins at the same tested levels, as well as increase in early apoptotic or apoptotic/necrotic cells with increase of caspases 3/7 activation. However, stronger effects were observed after BEA exposure than for EN B (Manyes et al., 2018).

5. Conclusions

To sum up, transcriptomic changes in Jurkat cells are revealed at genes codifying mitochondria related proteins after BEA end EN B mixture exposure at low levels during 24 h. The expression profile after mycotoxin mixture exposure was the opposite of those after individual and higher concentration exposures, showing a down-regulation of the expression of antioxidant activity related genes. Longer exposures of several months, as in adults the pool of mature T cells is relatively self-sufficient, and different concentrations and proportions of the emerging *Fusarium* mycotoxins, as they are found in food, should be studied in order to simulate chronic intake and perform a precise risk assessment.

Conflicts of interest

The authors declare no conflict of interest.

Acknowledgements

This work was supported by the Spanish Ministry of Science, Innovation and Universities (AGL2016-77610-R, BES-2014-068039 and BES-2017-081328).

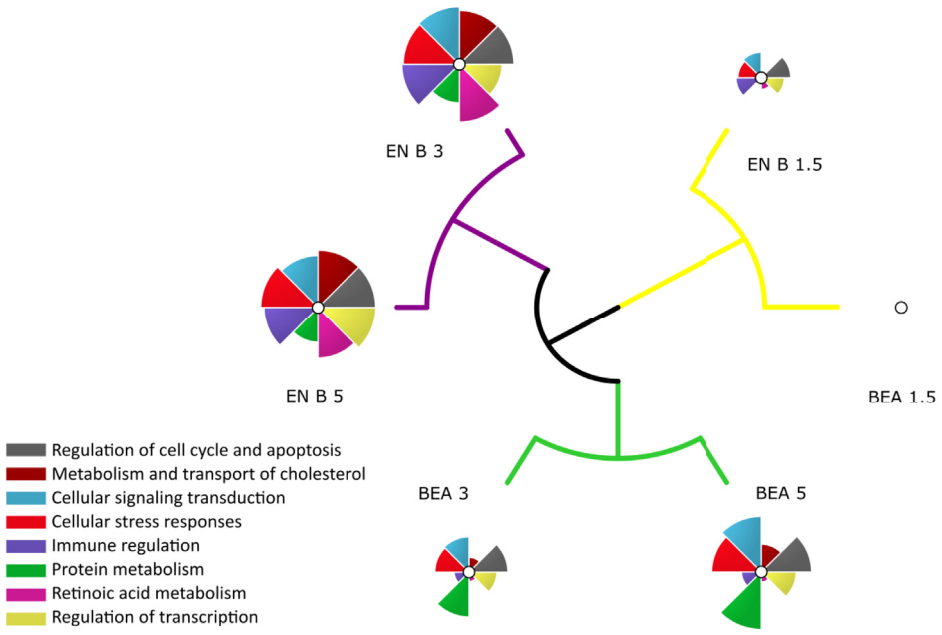

Fig. 2. ToxPi visualization of the effects in eight biological processes and molecular functions (GOs) after different exposure conditions (BEA 1.5 μM; BEA 3 μM; BEA 5 μM; EN B 1.5 μM; EN B 3 μM; EN B 5 μM) in human Jurkat T cells. Pie graphs represent different exposure conditions, while each colored pie piece represents one single GO item, which dimension reflects the ToxPi score.

Transparency document

Transparency document related to this article can be found online at https://doi.org/10.1016/j.fct.2019.05.018

References

Alonso-Garrido, M., Escrivá, L., Manyes, L., Font, G., 2018. Enniatin B induces expression changes in the electron transport chain pathway related genes in lymphoblastic T-cell line. Food Chem. Toxicol. 121, 437–443.

Banda, M., Bommineni, A., Thomas, R.A., Luckinbill, L.S., Tucker, J.D., 2008. Evaluation and validation of housekeeping genes in response to ionizing radiation and chemical exposure for normalizing RNA expression in real-time PCR. Mutat. Res. Genet. Toxicol. Environ. Mutagen 649, 126–134.

Cheng, H.Y., Gaddis, D.E., Wu, R., McSkimming, C., Haynes, L.D., Taylor, A.M., McNamara, C.A., Sorci-Thomas, M., Hedrick, C.C., 2016. Loss of ABCG1 influences regulatory T cell differentiation and atherosclerosis. J. Clin. Investig. 126, 3236–3246.

Damen, M.S.M.A., Dos Santos, J.C., Hermsen, R., Adam van der Vliet, J., Netea, M.G., Riksen, N.P., Dinarello, C.A., Joosten, L.A.B., Heinhuis, B., 2018. Interleukin-32 up-regulates the expression of ABCA1 and ABCG1 resulting in reduced intracellular lipid concentrations in primary human hepatocytes. Atherosclerosis 271, 193–202.

Devreese, M., De Baere, S., De Backer, P., Croubels, S., 2013. Quantitative determination of the Fusarium mycotoxins beauvericin, enniatin A, A1, B and B1 in pig plasma using high performance liquid chromatography-tandem mass spectrometry. Talanta 106, 212–219.

EFSA CONTAM Panel (EFSA Panel on Contaminants in the Food Chain), 2014. Scientific Opinion on the risks to human and animal health related to the presence of beauvericin and enniatins in food and feed. EFSA J. https://doi.org/10.2903/j.efsa.2014.3802. 2014, 12(8):3802, 174.

Escrivá, L., Jennen, D., Caiment, F., Manyes, L., 2018. Transcriptomic study of the toxic mechanism triggered by Beauvericine in Jurkat cells. Toxicol. Lett. 284, 213–221.

Fraeyman, S., Croubels, S., Devreese, M., Antonissen, G., 2017. Emerging Fusarium and Alternaria mycotoxins: occurrence, toxicity and toxicokinetics. Toxins 9, 228.

Ge, H., Zhang, F., Duan, P., Zhu, N., Zhang, 2, Ye, F., Shan, D., Chen, H., Lu, X., Zhu, C., Ge 2, Lin, Z., 2017. Mitochondrial Uncoupling Protein 2 in human cumulus cells is associated with regulating autophagy and apoptosis, maintaining gap junction integrity and progesterone synthesis. Mol. Cell. Endocrinol. 443, 128–137.

Hu, J., Yao, H., Gan, F., Tokarski, A., Wang, Y., 2012. Interaction of OKL38 and p53 in regulating mitochondrial structure and function. PLoS One 7, e43362.

Huang, C.-H., Wang, F.-T., Chan, W.-H., 2018. Enniatin B1 exerts embryotoxic effects on mouse blastocysts and induces oxidative stress and immunotoxicity during embryo development. Environ. Toxicol. 2018, 1–12.

Jonsson, M., Jestoi, M., Anthoni, M., Welling, A., Loivamaa, I., Hallikainen, V., Kankainen, M., Lysøe, E., Koivisto, P., Peltonen, K., 2016. Fusarium mycotoxin enniatin B: cytotoxic effects and changes in gene expression profile. Toxicol. Vitro 34, 309–320.

Joseph, P., 2017. Transcriptomics in toxicology. Food Chem. Toxicol. 109, 650–662.

Korkalainen, M., Taubel, M., Naarala, J., Kirjavainen, P., Koistinen, A., Hyvarinen, A., Komulainen, H., Viluksela, M., 2017. Synergistic proinflammatory interactions of microbial toxins and structural components characteristic to moisture-damaged buildings. Indoor Air 27, 13–23.

Mallebrera, B., Juan-Garcia, A., Font, G., Ruiz, M.-J., 2016. Mechanisms of beauvericin toxicity and antioxidant cellular defense. Toxicol. Lett. 246, 28–34.

Manyes, L., Escrivá, L., Ruiz, M.J., Juan-García, A., 2018. Beauvericin and enniatin B effects on a human lymphoblastoid Jurkat T-cell model. Food Chem. Toxicol. 115, 127–135.

Martínez-Gac, L., Marqués, M., García, Z., Campanero, M.R., Carrera, A.C., 2004. Control of cyclin G2 mRNA expression by forkhead transcription factors: novel mechanism for cell cycle control by phosphoinositide 3-kinase and forkhead. Mol. Cell. Biol. 24, 2181–2189.

Nouws, J., Goswami, A.V., Bestwick, M., McCann, B.J., Surovtseva, Y.V., Shadel, G.S., 2016. Mitochondrial ribosomal protein L12 is required for POLRMT stability and exists as two forms generated by alternative proteolysis during import. J. Biol. Chem. 291, 989–997.

Ogasawara, N., Kudo, T., Sato, M., Kawasaki, Y., Yonezawa, S., Takahashi, S., Miyagi, Y., Natori, Y., Sugiyama, A., 2018. Reduction of membrane protein CRIM1 decreases E-cadherin and increases claudin-1 and MMPs, enhancing the migration and invasion of renal carcinoma cells. Biol. Pharm. Bull. 41, 604–611.

Oliveira, B.A.P., Pinhel, M.A.S., Nicoletti, C.F., Oliveira, C.C., Quinhoneiro, D.C.G., Noronha, N.Y., Marchini, J.S., Marchry, A.J., Junior, W.S., Nonino, C.B., 2017. UCP1 and UCP3 expression is associated with lipid and carbohydrate oxidation and body composition. PLoS One 11, e0150811.

Pan, X.N., Chen, J.J., Wang, L.X., Xiao, R.Z., Liu, L.L., Fang, Z.G., Liu, Q., Long, Z.J., Lin, D.J., 2014. Inhibition of c-Myc overcomes cytotoxic drug resistance in acute myeloid leukemia cells by promoting differentiation. PLoS One 9, e105381.

Prosperini, A., Berrada, H., Ruiz, M.J., Caloni, F., Coccini, T., Spicer, L.J., Perego, M.C., Lafranconi, A., 2017. A review of the mycotoxin enniatin B. Front. Public Health 5, 304.

Quintana, A., Hoth, M., 2012. Mitochondrial dynamics and their impact on T cell function. Cell Calcium 52, 57–63.

Schmeits, P.C., Volger, O.L., Zandvliet, E.T., van Loveren, H., Peijnenburg, A.A., Hendriksen, P.J., 2017. Assessment of the usefulness of the murine cytotoxic T cell line CTLL-2 for immunotoxicity screening by transcriptomics. Toxicol. Lett. 217, 1–13.

Schoevers, E.J., Santos, R.R., Fink-Gremmels, J., Roelena, B.A.J., 2016. Toxicity of beauvericin on porcine oocyte maturation and preimplantation embryo development. Reprod. Toxicol. 65, 159–169.

Shao, J., Berger, L.F., Hendriksen, P.J.M., Peijnenburg, A.A.C.M., van Loveren, H., Volger, O.L., 2014. Transcriptome-based functional classifiers for direct immunotoxicity. Arch. Toxicol. 88, 673–689.

Smith, M.-C., Madec, S., Coton, E., Hymery, N., 2016. Natural Co-occurrence of mycotoxins in foods and feeds and their in vitro combined toxicological effects. Toxins 8, 94.

Stanciu, O., Juan, C., Miere, D., Loghin, F., Mañes, J., 2017. Occurrence and co-occurrence of Fusarium mycotoxins in wheat grains and wheat flour from Romania. Food Control 73, 147–155.

Whitaker-Menezes, D., Martinez-Outschoorn, U.E., Flomenberg, N., Birbe, R.C., Witkiewicz, A.K., Howell, A., Pavlides, S., Tsirigos, A., Ertel, A., Pestell, R.G., Broda, P., Minetti, C., Lisanti, M.P., Sotgia, F., 2011. Hyperactivation of oxidative mitochondrial metabolism in epithelial cancer cells in situ: visualizing the therapeutic effects of metformin in tumor tissue. Cell Cycle 10, 4047–4064.

Wilson, V.S., Keshava, N., Hester, S., Segal, D., Chiu, W., Thompson, C.M., Euling, S.Y., 2013. Utilizing toxicogenomic data to understand chemical mechanism of action in risk assessment. Toxicol. Appl. Pharmacol. 271, 299–308.
Ye, J., Coulouris, G., Zaretskaya, I., Cutcutache, I., Rozen, S., Madden, T., 2013. Primer-BLAST: a tool to design target-specific primers for polymerase chain reaction. BMC Bioinf. 13, 134.
Zhang, B., Liu, S.Q., Li, C., Lykken, E., Jiang, S., Wong, E., Zhongfen, T., Zhu, B., Wan, Y., Li, Q.-J., 2016. MicroRNA-23a curbs necrosis during early T cell activation by enforcing intracellular reactive oxygen species equilibrium. Immunity 44, 568–581.